

# 1D/2D carbon nanotube/graphene nanosheet composite anodes fabricated using electrophoretic assembly

Seung-Deok Seo, In-Sung Hwang, Seung-Hun Lee, Hyun-Woo Shim, Dong-Wan Kim \*

*Department of Materials Science & Engineering, Ajou University, Woncheon-dong, San 5, Yeongtong-gu, Suwon 443-749, Republic of Korea*

Received 17 November 2011; received in revised form 30 November 2011; accepted 30 November 2011

Available online 8 December 2011

## Abstract

This study examines the direct assembly of hybrid graphene nanosheets (GNSs) and multiwalled carbon nanotubes (MWCNTs) onto Ni current collectors in the presence of an electric field. The dissociation of Ni nitrate salt, which provides ions to charge the GNSs and MWCNTs positively, facilitates the homogeneous dispersion of each powder and assists in electrophoretic deposition. Direct assembly by this electrophoretic deposition results in the effective packing of GNS/MWCNT composites without any appreciable agglomeration, which is desirable for achieving high electrochemical performance of the composite electrodes in Li-ion batteries. Hence, GNS/MWCNT composite electrodes exhibit higher specific capacity compared to electrodes made of pure GNSs or MWCNTs owing to better realization of electrolyte permeability and Li-ion transfer. © 2011 Elsevier Ltd and Techna Group S.r.l. All rights reserved.

**Keywords:** Multiwalled carbon nanotubes; Graphene nanosheets; Electrophoretic deposition; Composite electrode; Li ion batteries

## 1. Introduction

Recently, carbon-based nanostructures have been studied intensively on material platforms for use in applications such as hydrogen storage devices, fuel cells, and Li-ion batteries [1,2]. Among the nanostructures, two-dimensional (2D) graphene nanosheets (GNSs) are very promising materials for next generation solid electrodes owing to their high surface area, superior conductivity, high porosity, and other interesting properties. However, in applications of or in the fabrication of GNS-based devices, the GNSs are easily agglomerated by strong van der Waals interaction; this agglomeration reduces the active area of the GNSs, resulting in low device performance [3].

To overcome the above-mentioned drawback, the use of composites of GNSs and other carbon-based nanostructures has been proposed. Yoo et al. reported high reversibility in the Li-storage properties of carbon-based composites such as the combination of GNSs and 1D carbon nanotubes (CNTs) or fullerenes (C<sub>60</sub>) [4]. The specific capacities of these GNS composites increased up to 730 mAh g<sup>-1</sup> and 784 mAh g<sup>-1</sup>,

respectively. The hierarchical GNS–CNT architecture was remarkably promising as a material platform for enhanced capacitive performance [5]. Additionally, the CNT/graphite hybrid composite shows high electron conductivity [6]. The above-mentioned previously reported results have been considered remarkably useful for the preparation of composite nanostructures for various applications such as high-performance electronic and energy storage devices.

In this study, GNSs were prepared by the electrochemical exfoliation method. A uniform composite film on Ni foil was fabricated by mixing 2D GNSs and 1D MWCNTs with controlled weight ratios by using a simple and inexpensive electrophoretic deposition process. The electrochemical performances of the GNS/MWCNT composite films were evaluated for use in the anode of Li-ion batteries.

## 2. Experimental procedure

The MWCNT powders (Hanwha Nanotech Co., Ltd.) were chemically treated with strong carboxyl acid for purification and surface modification. A 2 g sample of MWCNTs was heated to reflux (110 °C) in a 3:1 H<sub>2</sub>SO<sub>4</sub>:HNO<sub>3</sub> solution for 30 min. After washing the treated sample, the black product was dried at 80 °C under vacuum. For the preparation of GNSs, a flexible graphite sheet, Grafoil® (0.25 mm thick, GrafTech)

\* Corresponding author. Tel.: +82 31 219 2468; fax: +82 31 219 1612.

E-mail address: [dwkim@ajou.ac.kr](mailto:dwkim@ajou.ac.kr) (D.-W. Kim).

was used the starting material for the stationary anode. A copper foil (25  $\mu\text{m}$  thick, Aldrich) supported by a glass plate, was used as the counter electrode with a separation of 2 cm. For the electrolytic exfoliation, 0.001 M of an aqueous electrolyte containing PSS (molecular weight = 70,000, Aldrich) was used [7]. The constant current between the two electrodes was set at 300 mA for 1 h, using a DC power supply (model E3612A, Agilent). The peeled flakes could be clearly observed based on the surface of the anodes, forming black slurry with the electrolyte during the electrolytic exfoliation process. Subsequently, the exfoliated graphene slurry was washed with water and ethanol, and then dried in a vacuum oven at 60  $^{\circ}\text{C}$  for 2 h. The evidence of the GNSs formation was confirmed by transmission electron microscopy (TEM, JEM-2100, JEOL), and high resolution TEM (HRTEM), as shown in Fig. 1a and b. A large portion of the sheets were a few layers of graphene, with a thin thickness of 3 nm, based on observations at their edge region, corresponding to an approximate 1–5 layer stacking of the monatomic graphene sheets.

The electrophoretic deposition process is shown Fig. 1c. The Ni foil (thickness of 25  $\mu\text{m}$ , Aldrich) and Al foil (thickness of 16  $\mu\text{m}$ ) were used as the cathode and anode, respectively. Both electrodes were separated by 1 cm. Fabrication of the GNS and MWCNT composites was completed using the as-prepared GNSs and acid-treated MWCNTs, which were homogeneously dispersed and mixed in a bath containing isopropyl alcohol

(IPA) with various weigh ratios using an ultrasonic generator (VCX 500, Sonics & Materials, Inc.). Following sonication, 4 mg of  $\text{Ni}(\text{NO}_3)_2$  was added to suspension. A constant voltage of 100 V was applied between the working and counter electrodes using a DC power supply for 10 min [8,9]. After deposition, the sample was dried at 80  $^{\circ}\text{C}$  under vacuum for 4 h.

The morphologies and crystal structures were characterized and analyzed using field emission scanning electron microscopy (FESEM, JSM-6330F, JEOL) and X-ray diffraction (XRD, D/max-2500V/PC, Rigaku). Additionally, the mass of the films was measured by a microbalance (0.1  $\mu\text{g}$ , model UMT5, Mettler Toledo).

The electrochemical performance was evaluated by Swagelok-type half-cells. The half-cells consist of a Li metal foil (negative electrode), separator film and GNS/MWCNT film coated Ni foil (positive electrode). The GNS–MWCNT composites on the Ni foil were diced disk-shape (diameter: 10 mm), which was directly used as an anode for the Li-ion batteries. A separator film of Celgard 2400 and liquid electrolyte (ethylene carbonate and dimethyl carbonate (1:1 by volume) with 1.0 M  $\text{LiPF}_6$ ) (Techno Semichem Co., Ltd.) was loaded between the two cell electrodes. The electrochemical properties of the assembled cells were evaluated in a voltage window between 0.01 and 2.0 V with various current rates of 0.2C, 0.5C and 1C using an automatic battery cycler (WBCS 3000, WonaTech Co., Ltd.).

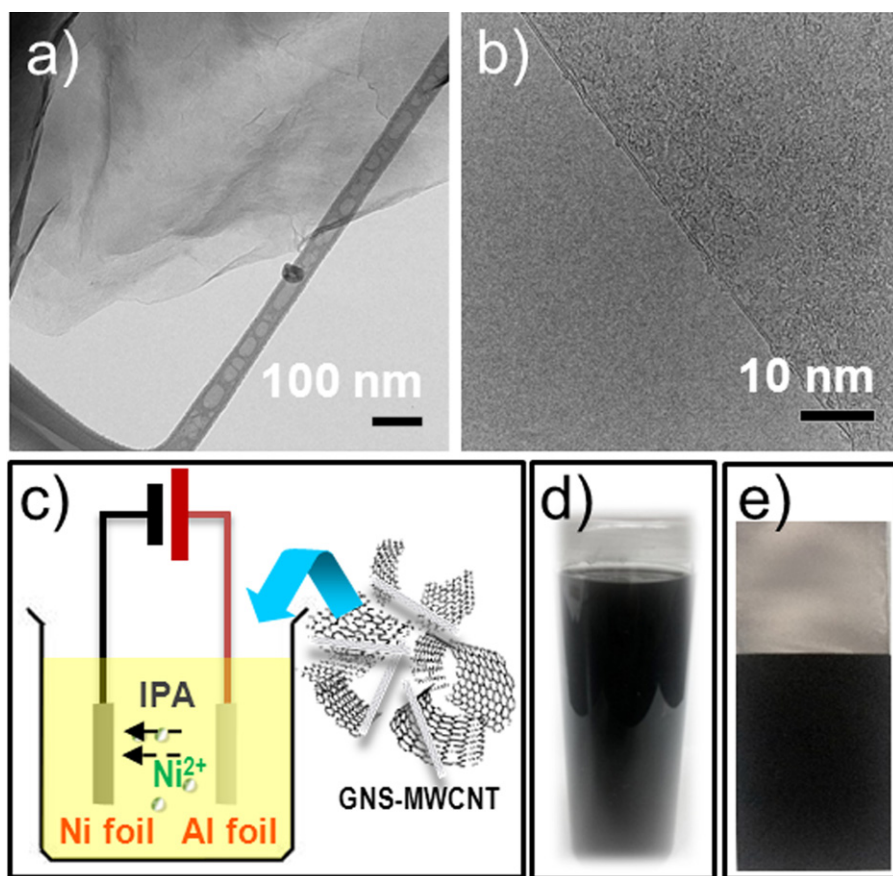


Fig. 1. (a and b) Typical TEM and HRTEM images of as-exfoliated GNSs, respectively. (c) Schematic representation of the electrophoretic deposition process. (d and e) Digital camera images of the 60G40C sample dispersed in IPA and 60G40C film electrophoretically deposited on Ni foil, respectively.

### 3. Results and discussion

Fig. 1d shows a digital image of the dispersed GNS/MWCNT composite in IPA. The black solution was well dispersed and very stable for several months without adding surfactants or polymers. The GNS/MWCNT composite was formed using a co-electrophoretic deposition process with various weight ratios. For simplicity, GNS/MWCNT composites prepared by weight ratio of 100:0, 80:20, 60:40, 40:60, 20:80 and 0:100 will be referred as “100G,” “80G20C,” “60G40C,” “40G60C,” “20G80C,” and “100C,” respectively. A large scale GNS/MWCNT composite film on Ni foil was obtained using a highly dispersed solution, which was advantageous in fabricating uniformly deposited composite films (Fig. 1e). Acid-treated MWCNTs have a slightly negative surface charge [10] resulting in relatively low-density films formed at the anode (Al foil) without Ni nitrate salt. However,

the small addition of Ni nitrate salt and the resultant  $\text{Ni}^{2+}$  ions provide positive charges to both the MWCNTs and GNSs. As a result, the hybrid GNS/MWCNT composite films were successfully fabricated on the cathode (Ni foil) in the presence of an electric field, as shown in Fig. 1e.

The XRD patterns of the electrophoretic deposited GNS/CNT composite films on Ni foil are shown in Fig. 2a. From X-ray analysis, a broad graphite peak (0 0 2) was observed at angles of  $\sim 25^\circ$  in all samples. In Fig. 2a, the shaded region was expanded to further analyze the detail of the graphite (0 0 2) peak ranging from  $24^\circ$  to  $28^\circ$ . In the MWCNT sample, broad and low intensity peaks of graphite (0 0 2) were observed at  $\sim 25.8^\circ$ . However, with an increasing amount of GNSs, the graphite (0 0 2) peak was slightly shifted to  $\sim 26.5^\circ$ . The relative intensity of the graphite peak (0 0 2) was also increased. The positive peak shift could be explained by the difference of the d-spacing value of the MWCNTs and GNSs. It

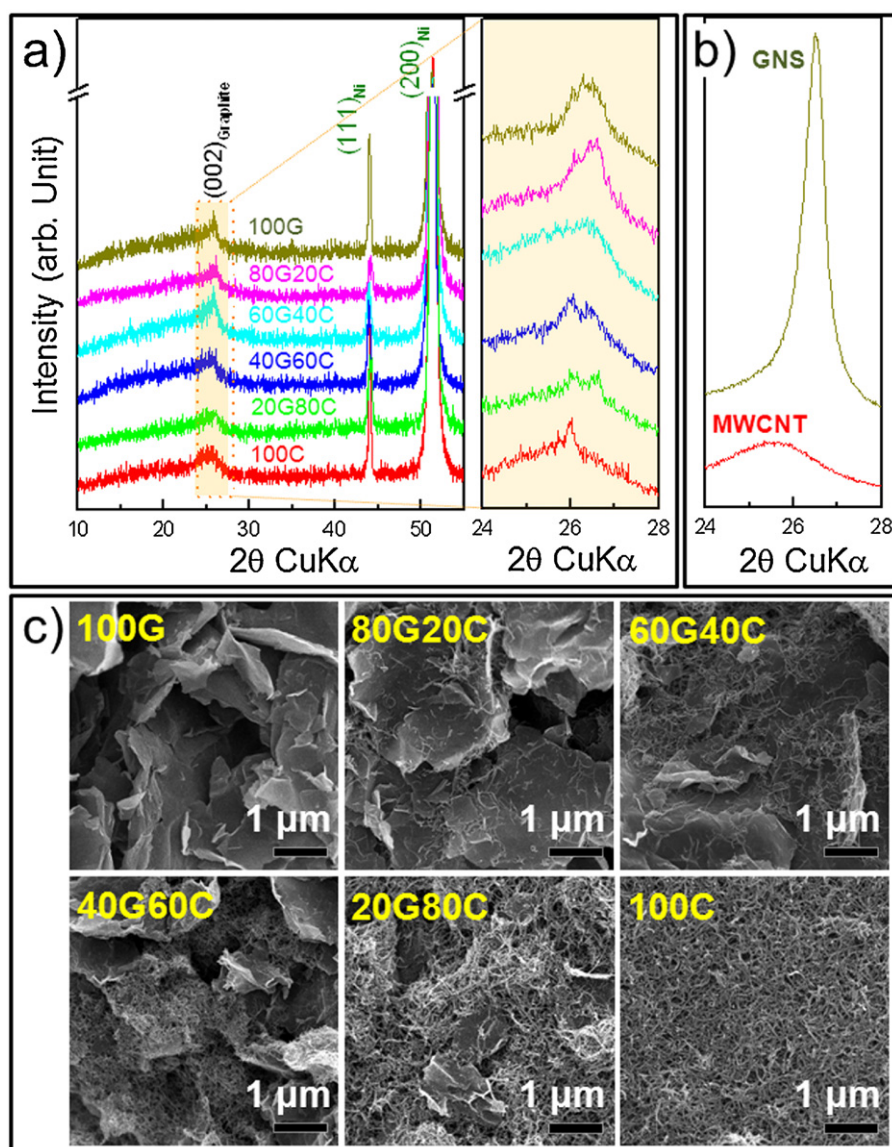


Fig. 2. XRD patterns of the (a) as-prepared composite films on Ni foil with various GNS/MWCNT weight ratios. (b) XRD patterns of the GNS and MWCNT powders. (c) Typical FESEM images of composite films with various GNS/MWCNT weight ratios.



can be postulated that the GNS has a smaller d-spacing value than the MWCNT sample. To confirm the above results, XRD analysis of the as-prepared GNSs and acid-treated MWCNT powders was conducted (Fig. 2b). The acid-treated MWCNT powder shows a broad graphite (0 0 2) peak. A sharp and relatively high intensity (0 0 2) peak of the as-prepared GNS powders was detected at relatively higher angle,  $\sim 26.5^\circ$  rather than that of MWCNT powders at  $\sim 25.8^\circ$ . These two peaks observed at  $26.5^\circ$  and  $25.8^\circ$  correspond to 3.35 Å and 3.45 Å of d-spacing, which are in good agreement with 3.40 Å and 3.44 Å of reported GNS and MWCNT, respectively [11,12]. Therefore, it can be suggested that GNS/MWCNT composite films with various GNS/MWCNT ratios were systematically formed on Ni foil using electrophoretic deposition. The SEM images of the GNS/MWCNT composites were shown in Fig. 2c. The morphology of the as-prepared GNSs shows a thin sheet shape. The acid-treated MWCNTs were 15 nm in thickness and several micrometers long. It was also confirmed that the 1D MWCNTs were well dispersed onto the 2D GNSs without any appreciable aggregations in each GNS/MWCNT composite.

Detailed verification of the composite morphology was performed by HRTEM analysis. The typical HRTEM images of the 60G40C samples were shown in Fig. 3. In Fig. 3, the individual MWCNTs were uniformly attached to the GNSs without agglomeration. The inset of Fig. 3 shows a schematic illustration of the hybrid 1D/2D MWCNT/GNS composites.

After dicing the GNS/MWCNT composite film, the weight of the active materials was measured precisely. The thickness of the GNS/MWCNT films on Ni foil was  $\sim 2 \mu\text{m}$ , and the average weight was  $\sim 200 \mu\text{g cm}^{-2}$ . The typical galvanostatic cycling performance of 100G, 60G40C and 100C at various current rates of 0.2C, 0.5C and 1C (based on the graphite's theoretical

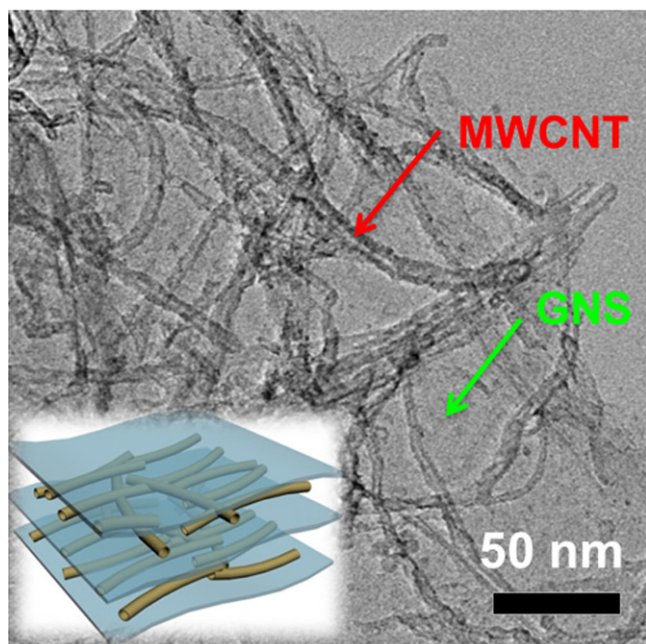


Fig. 3. Typical HRTEM image of 60G40C composites. Inset of the figure demonstrates the schematic illustration of the GNS/MWCNT composites with uniform mixing.

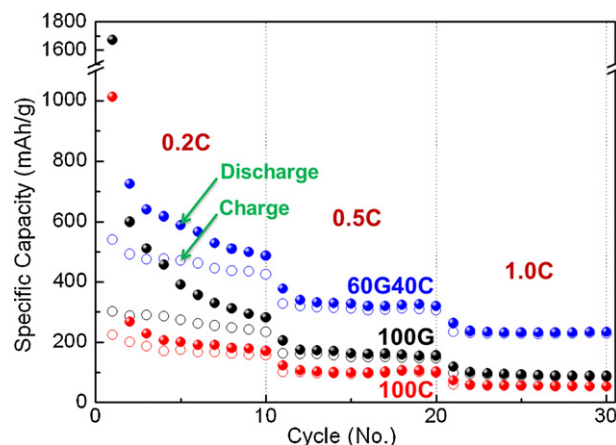


Fig. 4. Cycling performance of the GNS/MWCNT composite electrodes at various current rates. (Filled and empty circle correspond to the discharge and charge capacities of each sample, respectively.)

capacity  $372 \text{ mAh g}^{-1}$  by the insertion reaction, formation of  $\text{LiC}_6$ ) is shown in Fig. 4. At 0.2C, the first discharge cycles of 100G, 60G40C, 100C show high specific capacity of  $\sim 1700$ ,  $2200$ ,  $1000 \text{ mAh g}^{-1}$ , respectively. At the second discharge cycle, the values decreased to  $600$ ,  $720$  and  $280 \text{ mAh g}^{-1}$ . The specific capacity values were dramatically reduced after the first discharge. Carbon based materials show a large irreversibility following the first cycle due to the formation of a solid electrolyte interface (SEI) film on the surface and the residual oxygen-containing functional groups, which causes the loss of capacity [13–15]. After 10 cycles, the discharge capacity of the 100G, 60G40C, 100C samples were  $282$ ,  $485$ ,  $170 \text{ mAh g}^{-1}$ , respectively.

Importantly, GNS and MWCNT electrodes have a lower capacity than the theoretical capacity of graphite but the charge and discharge capacity of 60G40C was much higher than other samples ( $330$  and  $230 \text{ mAh g}^{-1}$  at  $0.5\text{C}$  and  $1.0\text{C}$ , respectively) at various current rates. Enhanced cycling performance was explained by a less agglomerated configuration in the GNS/CNT composites, resulting in efficient permeability of the electrolyte and lithium ions. CNTs usually form bundles, limiting their surface area and graphene nanosheets are likely to agglomerate through van der Waals interactions. It would be difficult for electrolyte to access the pores, especially at a high current rate. In the GNS/CNT composite, CNT can serve as a spacer between the GNS providing much higher porosity and efficient diffusion pathways for the electrolyte ions [16]. Therefore, the presented GNS/MWCNT composites fabricated using electrophoretic assembly enable marked improvements in the electrochemical performance of both GNSs and MWCNTs, even without any conductive additives and cohesive polymer binder.

#### 4. Conclusions

The direct assembly of GNS/MWCNT composites with various weight ratios using the cost-effective electrophoretic deposition process on a metal substrate was demonstrated

without binders. From FESEM and HRTEM, the 2D GNS and 1D MWCNT samples were mixed homogeneously without any agglomeration. Galvanostatic cycling of the GNS/MWCNT composite was performed at various current rates. The 60G40C composite sample shows higher capacity than GNSs and MWCNTs. It was suggested that the Li ions and electrons move easily along the homogeneously mixed GNS and MWCNT matrix due to the less agglomerated configuration.

## Acknowledgement

This work was supported by the National Research Foundation of Korea (NRF) grant funded by the Korea Government (MEST) (Nos. 2011-0019119 and 2010-0029617).

## References

- [1] A.K. Geim, K.S. Novoselov, The rise of graphene, *Nature* 6 (2007) 183–191.
- [2] J. Wu, W. Pisula, K. Mullen, Graphenes as potential material for electronics, *Chem. Rev.* 107 (2007) 718–747.
- [3] H.W. Tien, Y.L. Huang, S.Y. Yang, J.Y. Wang, C.C.M. Ma, The production of graphene nanosheets decorated with silver nanoparticles for use in transparent, conductive films, *Carbon* 49 (2011) 1550–1560.
- [4] E. Yoo, J. Kim, E. Hosono, H.-S. Zhou, T. Kudo, I. Honma, Large reversible Li storage of graphene nanosheet families for use in rechargeable lithium ion batteries, *Nano Lett.* 8 (2008) 2277–2282.
- [5] S.Y. Yang, K.H. Chang, H.W. Tien, Y.F. Lee, S.M. Li, Y.S. Wang, J.Y. Wang, C.C.M. Ma, C.C. Hu, Design and tailoring of a hierarchical graphene–carbon nanotube architecture for supercapacitors, *J. Mater. Chem.* 21 (2011) 2374–2380.
- [6] D. Cai, M. Song, C. Xu, Highly conductive carbon-nanotube/graphite-oxide hybrid films, *Adv. Mater.* 20 (2008) 1706–1709.
- [7] G. Wang, B. Wang, J. Park, Y. Wang, B. Sun, J. Yao, Highly efficient and large-scale synthesis of graphene by electrolytic exfoliation, *Carbon* 47 (2009) 3242–3246.
- [8] H. Ma, L. Zhang, J. Zhang, L. Zhang, N. Yao, B. Zhang, Electron field emission properties of carbon nanotubes-deposited flexible film, *Appl. Surf. Sci.* 251 (2005) 258–261.
- [9] D.W. Kim, D.H. Lee, B.K. Kim, H.J. Je, J.G. Park, Direct assembly of BaTiO<sub>3</sub>-poly(methyl methacrylate) nanocomposite films, *Macromol. Rapid Commun.* 27 (2006) 1821–1825.
- [10] C. Du, J. Yeh, N. Pan, Carbon nanotube thin films with ordered structures, *J. Mater. Chem.* 15 (2005) 548–550.
- [11] G. Wang, J. Yang, J. Park, X. Gou, B. Wang, H. Liu, J. Yao, Facile synthesis and characterization of graphene nanosheets, *J. Phys. Chem. C* 112 (2008) 8192–8195.
- [12] Z.Q. Tian, S.P. Jiang, Y.M. Liang, P.K. Shen, Synthesis and characterization of platinum catalysts on multiwalled carbon nanotubes by intermittent microwave irradiation for fuel cell applications, *J. Phys. Chem. B* 110 (2006) 5343–5350.
- [13] H. Zhou, S. Zhu, M. Hibino, I. Honma, M. Ichihara, Lithium storage in ordered mesoporous carbon (CMK-3) with high reversible specific energy capacity and good cycling performance, *Adv. Mater.* 15 (2003) 2107–2111.
- [14] D. Aurbach, Review of selected electrode–solution interactions which determine the performance of Li and Li ion batteries, *J. Power Sources* 89 (2000) 206–218.
- [15] W. Xing, J.R. Dahn, Study of irreversible capacities for Li insertion in hard and graphitic carbons, *J. Electrochem. Soc.* 144 (1997) 1195–1201.
- [16] Q. Cheng, J. Tang, J. Ma, H. Zhang, N. Shinya, L.C. Qin, Graphene and carbon nanotube composite electrodes for supercapacitors with ultra-high energy density, *Phys. Chem. Chem. Phys.* 13 (2011) 17615–17624.